NUCL SCI TECH (2018) 29:93
https://doi.org/10.1007/s41365-018-0442-9

Radionuclide concentrations in sand samples from riverbanks of Muzaffarabad, Azad Kashmir

Abdul Razzaq Khan[1] · Muhammad Rafique[1] · Abdul Jabbar[2] · Saeed Ur Rahman[3] · Muhammad Ikram Shahzad[4] · Muhammad Ejaiz Khan[1] · Mulaika Yasin[1]

Received: 14 May 2017 / Revised: 19 July 2017 / Accepted: 19 October 2017 / Published online: 28 May 2018

Abstract This paper presents the results of a radiological risk assessment arising from the presence of naturally occurring radionuclides in sand samples from three riverbanks in Muzaffarabad. The mean values obtained for ^{232}Th, ^{226}Ra, and ^{40}K were found to be 44.58 ± 3.34, 48.25 ± 1.77, and 239.92 ± 22.73 Bq kg^{-1}, respectively. To assess the uniformity of exposure, the radium equivalent activity (Ra_{eq}) was calculated and was found to be 130.47 ± 8.29 Bq kg^{-1}. The current reported value for Ra_{eq} is lower than the maximum permissible value, that is, 370 Bq kg^{-1}, and equivalent to a gamma dose of 1.5 mSv y^{-1}. To investigate the possible contribution to health risks of alpha particle exposure, the radon exhalation rate (RER) from the sand samples was determined. The mean RER for all the samples was found to be 335 mBq m^{-2} h^{-1}. About 43% of the samples were found to have an indoor excess lifetime cancer risk value slightly higher than recommended safety limit of 1, as proposed by the ICRP. A normalized parameter, the equivalent multiplicative factor, was defined and used to compare the current results with the findings of studies performed in other countries. Our findings are relevant to both human health and future environmental radiation monitoring.

Keywords Radiological risk · Radon exhalation rate · Absorbed dose rate · Hazard index · Annual effective dose

1 Introduction

If building materials, either of natural origin or formed from industrial by-products, have elevated levels of radioactivity, they can contribute to radiation exposure of the population. Almost all building materials with a rock or soil origin contain various amounts of radionuclides. Long-lived radionuclides with half-lives comparable to the age of the earth, e.g., those derived from either ^{238}U or ^{232}Th series and ^{40}K, can still be found today in the Earth's crust. ^{226}Ra has the greatest radiological importance in the ^{238}U decay series, causing it to be referenced very often instead of ^{238}U [1]. The consequences of radionuclides being present in building materials are twofold, that is, external irradiation of the body from direct gamma radiation and internal irradiation of the lung tissues from ^{222}Rn, ^{220}Rn (thoron), and its alpha-emitting progenies [2]. Human exposure arising from direct gamma radiation, called external exposure, is considered to be the largest external dose contributor to the world's population [3, 4]. Building materials with elevated levels of ^{226}Ra, ^{232}Th, and ^{40}K may be responsible for external doses.

On the other hand, internal exposure is mainly caused by alpha-emitting radionuclides. Radon (^{222}Rn), thoron (^{220}Rn) and their short-lived progenies are responsible for internal exposure. Since uranium is present in all types of building materials in trace amounts, with radon being its

✉ Muhammad Rafique
mrafique@gmail.com

[1] Department of Physics, University of Azad Jammu and Kashmir Muzaffarbad, Azad Kashmir 13100, Pakistan

[2] Health Physics Division, Pakistan Institute of Nuclear Science and Engineering (PINSTECH), Nilore, Islamabad 45650, Pakistan

[3] Department of Medical Physics, Nuclear Medicine, Oncology and Radiotherapy Institute, Islamabad, Pakistan

[4] Physics Division, Directorate of Science, PINSTECH, P.O. Nilore, Islamabad 45650, Pakistan

sixth decay product in series, the presence of radon within indoor environments is regarded as being natural. Although the main source of indoor radon (IR) is the underlying soil, in some cases the building materials may contribute significantly to the IR levels. As mentioned in the European Commission Radiation Protection 112 report, typical excess IR levels due to building materials are about 10–20 Bq m^{-3}, although this value may escalate and become greater than 1000 Bq m^{-3} in some rare circumstances. In addition to adding radon to the indoor environment, building materials are also believed to be the most significant source of indoor thoron (IT). However, the importance of IT is limited due to its short half-life, but its concentration solely depends upon the level of thorium in building materials [5]. While keeping the importance of radiological hazards in mind, as they relate to the presence of radionuclides in building materials, many researchers across the globe have conducted studies to identify and mitigate this problem [6–25]. Regarding the building materials themselves, sand is an integral part of many materials and it is usually formed by the weathering of rocks. Broadly, it is classified as pit sand, river sand, and sea sand. Sand from rivers in Muzaffarabad is commonly used for building. It is obtained from the banks or bed of the rivers. It consists of fine rounded grains.

The radon exhalation rate plays an important role in characterizing building materials and their contribution to indoor radon levels [26]. Within mineral grains ^{222}Rn is produced from the α-particle decay of ^{226}Ra. Since there are very few pore spaces, a large amount of radon remains within the mineral grains and only a small fraction of it can escape. During the radon emanation process, the radon escapes from the grains of the material into the pores [27, 28]. The fraction of radon escaping from the pore spaces is called the "emanation coefficient" (EC). Radon emanation depends upon different parameters including the ^{226}Ra distribution and amount within the grains, the water content within the pore spaces, the porosity, and the grain size [29, 30]. For different materials, the value of EC ranges from 0.05 to 0.7. In the case of sand EC ranges from 0.15 to 0.3 [31]. The fraction of radon reaching the surface of a building material is subject to diffusion and convective flow processes. This liberated quantity of radon per unit surface area of building material per unit time is called the "radon exhalation rate" (RER) [32].

The rationale of the current study was to recognize and compute the significant gamma emitting radionuclide's concentration in sand samples collected from three rivers in Muzaffarabad. The study of the radon exhalation rate and gamma spectroscopy of the sand samples can allow us to assess the radiological risk due to the inhalation of airborne radon emanating from the sand, building material, and external human exposure to gamma radiation originating from naturally occurring radionuclides. The radionuclide concentration is found using gamma-ray spectroscopy, while the radon exhalation rate is determined using the closed "CAN" technique [13, 15, 32].

2 Experimental procedures

2.1 Sample collection

The samples of sand were collected from the banks of the Neelum, Jhelum, and Kunhar rivers. A total of thirty sand samples were collected from along a 40-km stretch of each river. Ten sand samples were collected from each river. The study area thus spanned four districts, namely, Muzaffarabad, Hattian Bala, Neelum, and Mansehra (KPK). To collect a sand sample from a site, the upper sand layer was removed to access the sand that is local to that site. (The upper layers are subject to movement as a result of the action of water.) Then, the polythene bag was filled with sand and sealed after being indexed. Every sample bag was marked with a sample code. In this way, a total of 30 samples were collected, each from a different location. To find the coordinates of the sampling locations, a global positioning system (GPS) was used.

2.2 Sample preparation

Sand samples, weighing 200 g, were pretreated in the Solid State Nuclear Tracks Laboratory of the University of Azad Jammu and Kashmir. Initially, the samples were dried by exposing them to sunlight. The sand samples were sieved through a sieve with a mesh size of less than 0.16 mm. Samples were then placed in an oven at 110 °C for 4–6 h. After the removal of the moisture, the samples were then packed in a cylindrical polyethylene container. This container was airtight, so that secular equilibrium between the parent and daughter radionuclides was achieved within 1 month. At this point, each sample was placed in the detector to measure gamma-ray activity by using an HPGe detector.

2.3 Gamma spectrometric analysis

A PC-based high-resolution gamma spectrometry system was used for the radiometric analysis of the heat-treated sand samples [33]. This system used a high-purity germanium (HPGe) coaxial detector with an efficiency of 30%, relative to a NaI(Tl) detector. To reduce the effect of background noise, the detector was shielded by 15 cm lead with an inner lining of 3 mm copper and 4 mm tin [12, 18, 21, 34, 35]. The calibration of the system was performed experimentally using IAEA soil-326. The minimum detectable activity (MDA) for each of the radio

nuclides ^{226}Ra, ^{232}Th, ^{40}K, and ^{137}Cs was determined using the following equation:

$$\text{Minimum Detectable Activity (MDA)} = \frac{4.66(\text{Continum Counts} + \text{Background Peak Counts})^{\frac{1}{2}}}{\text{Sample Mass (kg)} \times \text{Efficiency} \times \text{Live time (s)} \times \text{Yield}} \quad (1)$$

where MDA is expressed in units of Bq kg^{-1} and 4.66 is the statistical coverage factor. The MDA values for radionuclides ^{226}Ra, ^{232}Th, ^{137}Cs, and ^{40}K were found to be 3.60, 2.25, 1.35, and 6.70 Bq kg^{-1}, respectively.

The activity concentrations due to ^{226}Ra, ^{232}Th, ^{137}Cs, and ^{40}K were calculated using the relationship proposed by Fredj et al. [36],

$$A_S(\text{Bq/sample}) = \frac{(\text{Net peak counts for sample} - \text{Background counts})}{\text{Counting time} \times \text{Detection efficiency} \times \text{Emission probability of - ray}} \quad (2)$$

3 Determination of gamma hazard indices and dose rate

Hazard indices, i.e., the radium equivalent activity, Ra_{eq}, internal, external hazard indices (H_{in}, H_{ex}), gamma index (I_γ), alpha index (I_α), and the representative level index I_r, were calculated to assess the radiation hazards associated with the individual sand samples. In addition, the absorbed dose rate, $\dot{D}$, in the air as well as the annual effective dose was estimated. The formulae for each of said indices and the dose rate (from Eqs. 3–10) are listed in Tables 1 and 2 [2, 4, 5, 37–40].

Since radionuclides are not uniformly distributed in building materials, a quantity known as the radium equivalent activity, Ra_{eq}, is defined to represent an equivalent uniform exposure to radiation due to radium, thorium, and potassium, in units of Bq/Kg. External hazards are defined for the external γ-radiation dose from building materials, while an internal hazard index is estimated to determine the radiation hazard to respiratory organs due to exposure to radon and its short-lived progenies. The gamma index (I_γ) and alpha index (I_α) are defined for the excess external gamma and excess α-radiation exposures, respectively. From a radiation safety perspective, a criterion defining an upper level for each of these parameters has been suggested. These criteria are shown in Table 1 in the second column, titled "Characteristics." The absorbed gamma dose rate in air and the annual effective dose due to radium, thorium, and potassium radionuclides are listed in Table 2.

4 Radon exhalation rate (RER) determination

The RER value was determined for thirty sand samples using the "CAN" technique [13, 15, 32]. To this end, all the samples were dried for 4 h in an oven at 110 °C. Samples, weighting 200 g, were put into plastic cans with a volume of 8.55 × 10^3 cm^3. Sheets of CR-39 detectors were cut into small strips measuring 2 × 2 cm^2 and placed inside the NRPB detector holder. Closing the holder prevents all radon decay products, as well as aerosol particles, from entering the active volume of the NRPB detector holder. That is, only radon can enter the sensitive volume and, when it decays, the resulting α-particles interact with the CR-39 detectors. The CR-39 detectors were tacked at the upper inner surface of cans 25 cm from the samples. The thirty cans were then hermetically sealed and left for 30 days. After exposure to radon for 30 days, the CR-39 detectors were retrieved and etched in 6 N NaOH at 80 °C. The etched detectors were cleaned with fresh tap water, and then the tracks were counted with the help of an optical microscope. The measured track densities were corrected for background contributions.

The calibration of the system was carried out at the PINSTECH Laboratory using the same method as that used by Matiullah [41]. Uranium ore samples of a known grade (to act as a source) were placed in plastic containers with a volume of 8.55 × 10^3 cm^3, and the CR-39 detectors, in NRPB-type holders, were exposed to the uranium samples for 4 weeks. After retrieval, the detectors were etched, as described above, to determine the track densities. A calibration factor of 2.713 tracks cm^{-2} h^{-1}/kBq m^{-3} was obtained and subsequently used to find the radon concentrations.

4.1 RER measurement methodology

The CR-39 detectors within the NRPB dosimeters were exposed for a period of 30 days, resulting in a variable radon exposure. The experimental setup for the measurement of the RER is shown in Fig. 1.

The effective detector exposure time to radon was calculated using the following relationship [32].

$$T_{\text{effective}} = \text{Total exposure time in Days } (t) - \text{Radon Mean Life Time } (\tau)\left[1 - e^{-\lambda t}\right] \quad (11)$$

Table 1 Formulae for determination of hazard indices

Hazard Index	Characteristics	References
Radium equivalent activity (Ra_{eq})		
$Ra_{eq} = A_{Ra} + (1.43 \times A_{Th}) + (0.077 \times A_K)$ (3)	The criterion $Ra_{eq} \leq 370$ Bq kg^{-1} should be met to guarantee that the external dose rate (D) remains less than or equal to 1.5 mGy y^{-1}	[37]
External Hazard Index (H_{ex})		
$H_{ex} = \frac{A_{Ra}}{370} + \frac{A_{Th}}{259} + \frac{A_K}{4810}$ (4)	To minimize radiation hazards, the External Hazard Index must be less than unity, i.e., $H_{ex} \leq 1$	[37]
Internal Hazard Index (H_{in})		
$H_{in} = \frac{A_{Ra}}{185} + \frac{A_{Th}}{259} + \frac{A_K}{4810}$ (5)	For minimizing radiation hazards, Internal Hazard Index must be less than unity for, i.e., $H_{in} \leq 1$	[37]
Gamma Index (I_γ)		
$I_\gamma = \frac{A_{Ra}}{300} + \frac{A_{Th}}{200} + \frac{A_K}{3000}$ (6)	For bulk material	[5]
	$I\gamma \leq 0.5 \Rightarrow D \leq 0.3$ mSv y^{-1}	[38]
	$I\gamma \leq 1.0 \Rightarrow D \leq 1.0$ mSv y^{-1}	
	For restricted material (tiles, etc.)	
	$I\gamma \leq 2 \Rightarrow D \leq 0.3$ mSv y^{-1}	
	$I\gamma \leq 6 \Rightarrow D \leq 1.0$ mSv y^{-1}	
Alpha Index (I_α)		
$I_\alpha = \frac{A_{Ra}}{200}$ (7)	Exemption level = 100 Bq kg^{-1}	[38, 39]
	Recommended upper level = 200 Bq kg^{-1}	
Representative level index (I_r)		
$I_r = \frac{A_{Ra}}{150} + \frac{A_{Th}}{100} + \frac{A_K}{1500}$ (8)	To keep radiation, hazard insignificant, I_r must be less than unity	[2]

A_{Ra}, A_{Th}, and A_K represent the activity concentrations of ^{226}Ra, ^{232}Th, and ^{40}K, respectively, in Bq kg^{-1}

Table 2 Dose rate, annual effective dose due to radionuclides ^{232}Th, ^{226} Ra, and ^{40}K

Hazard Index	Characteristics	References
Absorbed gamma dose rate in air (nGy h^{-1})		
$\dot{D} = (0.462 \times A_{Ra}) + (0.604 \times A_{Th}) + (0.0417 \times A_K)$ (9)	Assumption: All decay products of ^{226}Ra and ^{232}Th are in radioactive equilibrium with their precursors	[4]
Annual effective dose eq. E (mSv y^{-1})		
$E = Q \times T \times O \times \dot{D} \times 10^{-6}$ (10)	Q = 0.7 Sv Gy^{-1}	[40]
"Q" is a conversion coefficient, and "T" is the time in hours,	T = 8760 h in 1 year	
"D." is the dose rate, and "O" is the occupancy factor.	D. is in nGy h^{-1}	

where τ (radon mean life time) = 5.5 days, λ is ^{222}Rn decay constant.

Durrani and Ilic stated that this type of correction is needed only for a closed system [31].

The RER was determined using the following relationship [13, 15, 32].

$$(\mathrm{RER})_0 = \frac{C(t)[\omega + \lambda V/A]}{\left[1 - e^{-\left(\frac{\omega A}{V} + \lambda\right)t}\right]} \quad (12)$$

Equation (12) was corrected to account for the back-diffusion factor. The radon exhalation rate under back-diffusion conditions is given by Eq. 13 [32],

$$\mathrm{RER} = (\mathrm{RER})_0 - \omega\, C = (\mathrm{RER})_0 - \varepsilon\lambda Z_0 \quad (13)$$

where the surface area of the sample was denoted by A and, within the closed chamber, the volume of the void spaces was denoted by V. The radon accumulation time within chamber is denoted by t. Here, $\omega = \varepsilon\lambda Z_o$ was used for the back-diffusion constant depending upon the given material type. Z_o was the thickness of the sample. Parameter $C(t)$ represents the concentration of ^{222}Rn that has to be exhaled.

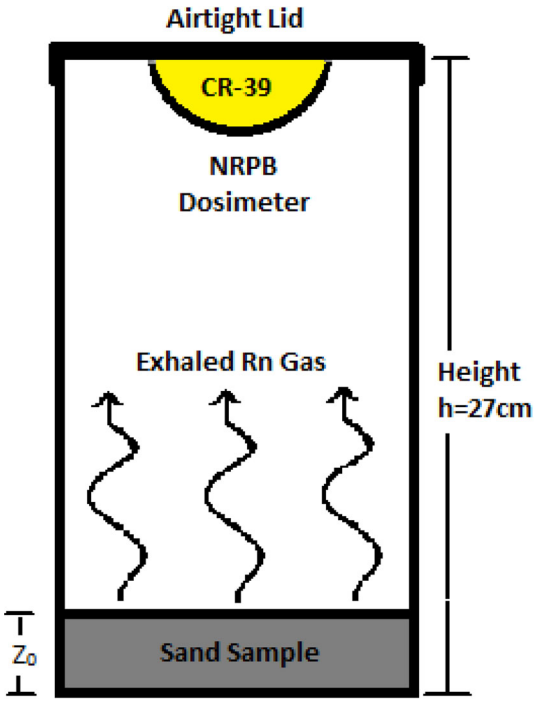

Fig. 1 (Color online) Experimental setup for measuring radon exhalation rate from sand samples [13, 15, 32]

5 Results and discussion

Ten samples were collected from banks of each of the Kunhar, Neelum, and Jhelum rivers and were then analyzed to determine the gamma-ray spectroscopy and radon exhalation rate. The obtained activity concentration (Bq kg^{-1}) of ^{232}Th, ^{226}Ra, and ^{40}K, on a dry weight basis,

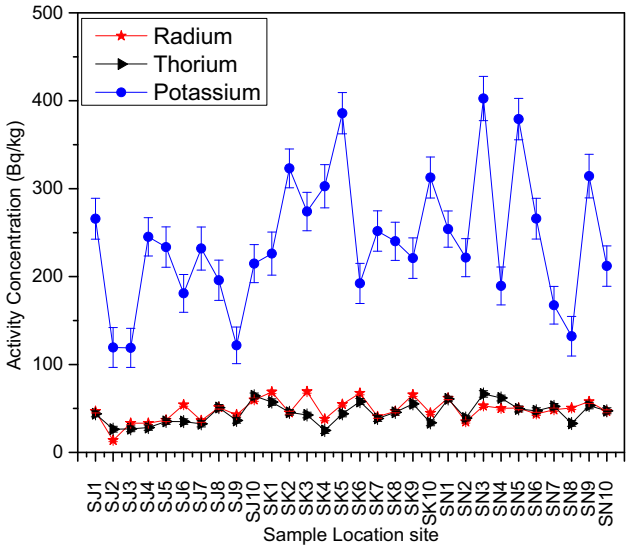

Fig. 2 (Color online) Activity concentration of ^{226}Ra, ^{232}Th, and ^{40}K in sand samples collected from the banks of the Jhelum, Kunhar, and Neelum rivers

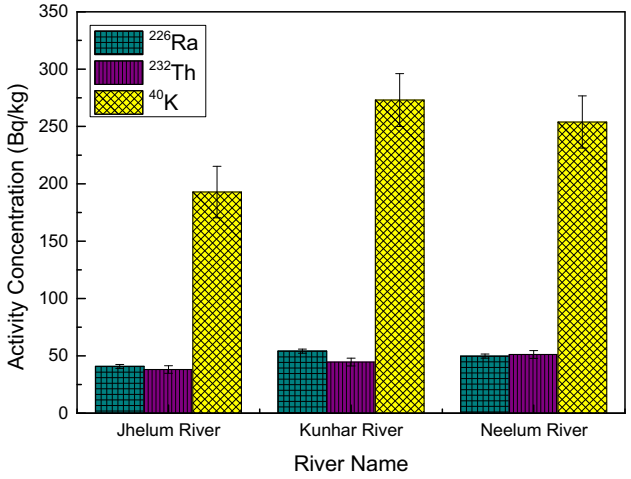

Fig. 3 (Color online) Average values of ^{226}Ra, ^{232}Th, and ^{40}K in sand samples

and the radon exhalation rate, for 30 samples of sand, are presented in Figs. 2, 3, 4, 5, 6, 7 and 8.

5.1 Determination of ^{226}Ra, ^{232}Th, and ^{40}K activity levels

For the sand samples collected from the Jhelum River, the activity concentration due to ^{226}Ra varied from 13.75 ± 1.55 to 59.87 ± 1.77 should be avoided $^{-1}$ with a mean value of 40.82 ± 1.71 Bq kg^{-1}. Similarly, the activity concentrations of ^{232}Th and ^{40}K varied from 26.48 ± 3.26 to 64.39 ± 3.35 with a mean value of 38.08 ± 3.28 Bq kg^{-1} and 118.99 ± 22.12 to 265.86 ± 23.28 Bq kg^{-1} with a mean value of 192.87 ± 22.41 Bq kg^{-1}, respectively. The radon exhalation rate varied from 139.89 to 411.04 mBq m^{-2} h^{-1} with a mean value of 289.92 mBq m^{-2} h^{-1}.

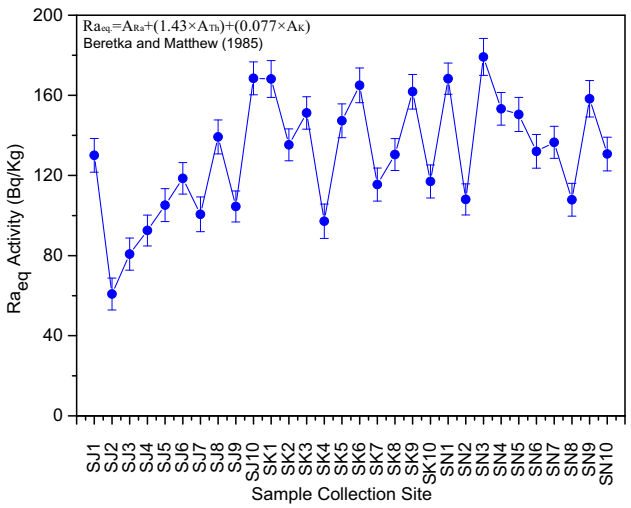

Fig. 4 Radium equivalent activity (Ra_{eq}) of sand samples

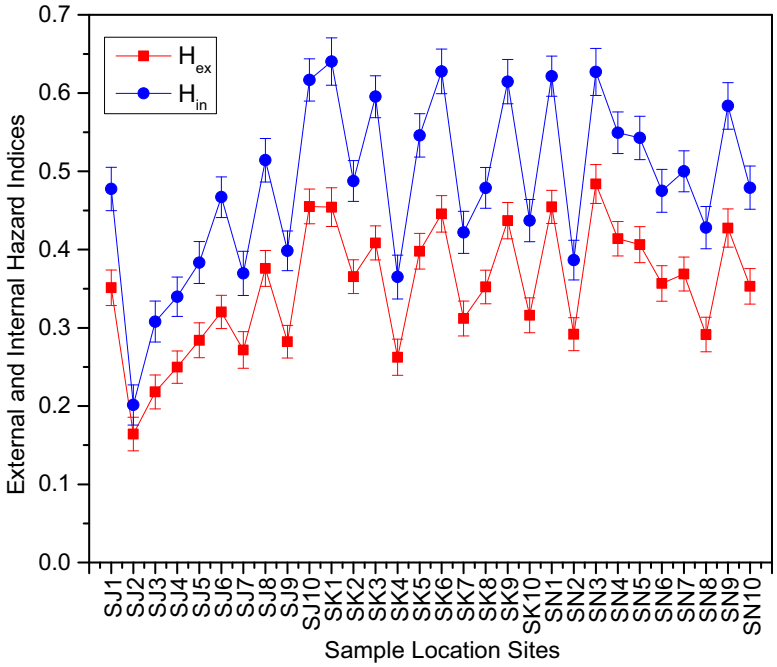

Fig. 5 External and internal hazard index

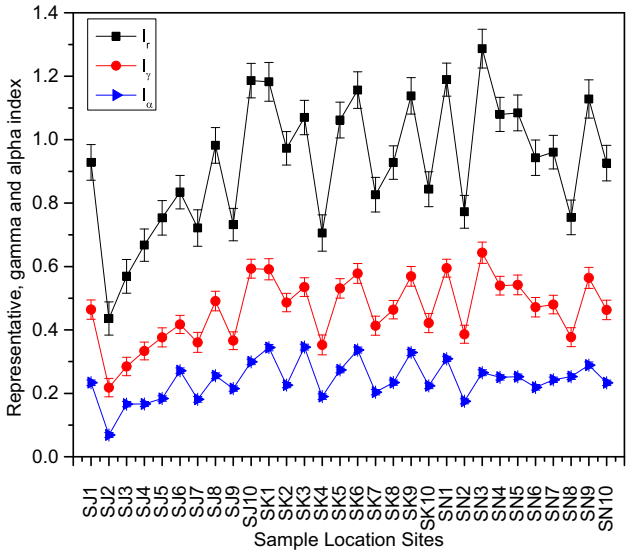

Fig. 6 Alpha, gamma, and representative level index for sand samples

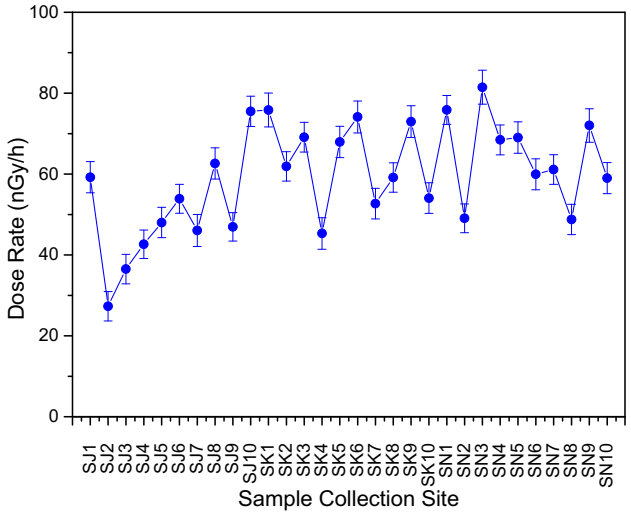

Fig. 7 Absorbed gamma dose rate in air (nGy h^{-1}) at point 1 m from the ground

Similarly, for those sand samples collected from the Kunhar River, the activity concentration due to ^{226}Ra varied from 37.95 ± 1.8 to 69.19 ± 1.83 Bq kg^{-1} with a mean value of 54.15 ± 1.81 Bq kg^{-1}. Similarly, the activity concentrations of ^{232}Th and ^{40}K varied from 25.09 ± 3.41 to 57.89 ± 3.48 Bq kg^{-1} with a mean value of 44.55 ± 3.36 Bq kg^{-1} and 192.31 ± 22.85 to 385.8 ± 23.47 Bq kg^{-1} with a mean value of 273.01 ± 23.03 Bq kg^{-1}, respectively. The radon exhalation rate varied from 261.94 to 504.31 mBq m^{-2} h^{-1} with a mean value of 375.24 mBq m^{-2} h^{-1}.

For the sand samples collected from the Neelum River, the activity concentration due to ^{226}Ra varied from 35.04 ± 1.61 to 61.78 ± 1.83 Bq kg^{-1} with a mean value of 49.78 ± 1.77 Bq kg^{-1}. Similarly, the activity concentrations of ^{232}Th and ^{40}K varied from 32.95 ± 3.27 to 66.55 ± 3.75 Bq kg^{-1} with a mean value of 51.14 ± 3.38 Bq kg^{-1} and 132.17 ± 22.48 to 402.59 ± 25.14 Bq kg^{-1} with a mean value of 253.9 ± 22.74 Bq kg^{-1}. The radon exhalation rate varied from 227.97 to 417.38 mBq m^{-2} h^{-1} with a mean value of 340.18 mBq m^{-2} h^{-1}. Figure 2 shows the average values for ^{226}Ra, ^{232}Th, and ^{40}K in sand samples collected from

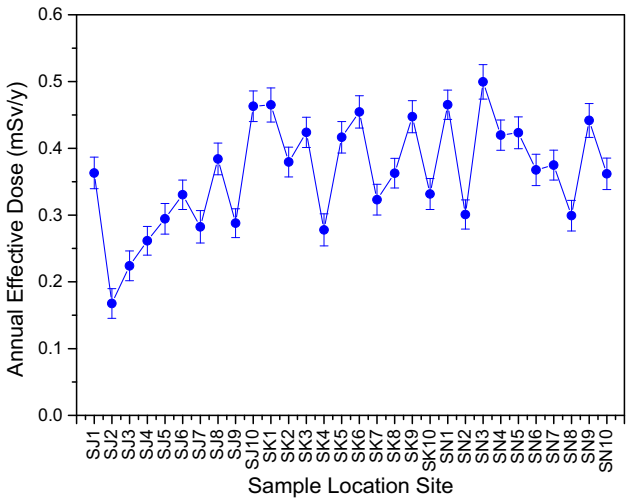

Fig. 8 Annual effective dose (mSv/y) of sand samples

the banks of the Jhelum, Kunhar, and Neelum rivers. Figure 3 shows the average values for ^{226}Ra, ^{232}Th, and ^{40}K in all three rivers.

5.2 Radium equivalent activities (Ra_{eq}) and radiological indices

The Ra_{eq} value of the sand samples collected from the banks of the Jhelum River varied from 60.81 ± 7.96 to 168.49 ± 8.23 Bq kg^{-1}with a mean value of 110.07 ± 8.13 Bq kg^{-1} (see Fig. 4).

The external (H_{ex}) and internal hazard (H_{in}) indices varied from 0.164 ± 0.0215 to 0.455 ± 0.0222 Bq kg^{-1} with a mean value of 0.297 ± 0.0219 Bq kg^{-1}and 0.201 ± 0.026 to 0.617 ± 0.027 Bq kg^{-1}with a mean value of 0.408 ± 0.0266 Bq kg^{-1}, respectively (see Fig. 5). The gamma (I_γ) and alpha (I_α) indices varied from 0.218 ± 0.029 to 0.593 ± 0.029 Bq kg^{-1} with a mean value of 0.391 ± 0.029 Bq kg^{-1}and 0.069 ± 0.008 to 0.299 ± 0.009 Bq kg^{-1} with a mean value of 0.204 ± 0.009 Bq/kg, respectively. The representative level index (I_r) varied from 0.436 ± 0.052 to 1.186 ± 0.054 Bq kg^{-1} with a mean value of 0.781 ± 0.053 Bq kg^{-1} (see Fig. 6).

For the sand samples collected from the banks of the Kunhar River, the radium equivalent activity was found to have a minimum value of 97.14 Bq/kg and a maximum value of 168.16 Bq/kg with an average value of 138.88 Bq/kg.

The values of the external (H_{ex}) and internal (H_{in}) hazard indices ranged from 0.26 ± 0.023 to 0.45 ± 0.025 with a mean value of 0.375 ± 0.022 and from 0.365 ± 0.28 to 0.640 ± 0.030 with a mean value of 0.521 ± 0.275, respectively. The gamma (I_γ) and alpha (I_α) indices varied from 0.353 ± 0.0312 to 0.591 ± 0.033 with a mean value of 0.559 ± 0.031 and from 0.190 ± 0.009 to 0.346 ± 0.009 with a mean vale of 0.270 ± 0.009. The value of the representative index ranged between 0.706 ± 0.057 and 1.182 ± 0.061 with an average value of 0.988 ± 0.056.

The value of Ra_{eq} for the sand samples collected from the Neelum River was found to be in a range of 107.876 ± 8.19 to 179.153 ± 9.22 Bq/kg, with an average value of 142.468 ± 8.358 Bq/kg (see Fig. 4).

The values of the external (H_{ex}) and internal (H_{in}) hazard indices in the sand samples taken from the River Neelum varied from 0.29 ± 0.022 to 0.48 ± 0.024 with a mean value of 0.38 ± 0.022 and from 0.39 ± 0.025 to 0.63 ± 0.030 with a mean value of 0.52 ± 0.027, respectively. The estimated values of the gamma (I_γ) and alpha (I_α) indices for the Neelum river varied from 0.38 ± 0.029 to 0.64 ± 0.034 with a mean value of 0.51 ± 0.030 and from 0.18 ± 0.008 to 0.31 ± 0.008 with a mean value of 0.25 ± 0.009. For this river, the value of the representative index varied from 0.75 ± 0.055 to 1.29 ± 0.061 with a mean value of 1.013 ± 0.055.

The overall value of Ra_{eq} for all of the 30 studied samples ranged from 60.81 ± 7.67 to 179.15 ± 9.22 Bq/kg with a mean value of 130.47 ± 8.29 Bq/kg (see Fig. 4).

The values of the external (H_{ex}) and internal (H_{in}) hazard indices for all the sand samples from all three rivers varied from 0.164 ± 0.021 to 0.484 ± 0.025 with a mean value of 0.352 ± 0.022 and from 0.201 ± 0.025 to 0.64 ± 0.03 with a mean value of 0.483 ± 0.027, respectively. The overall estimated ranges of the gamma (I_γ) and alpha (I_α) indices were found to be 0.218 ± 0.028, 0.644 ± 0.034 with a mean value of 0.464 ± 0.03 and 0.069 ± 0.008, and 0.346 ± 0.01 with a mean value of 0.241 ± 0.009. For all the samples, the value of the representative index ranged from 0.436 ± 0.051 to 1.287 ± 0.061 with a mean value of 0.927 ± 0.055.

For all the sand samples, the ^{40}K content was very much dependent on the location, with the lowest value being 118.9 Bq kg^{-1}, that being obtained for the sand sample collected from the bank of the Jhelum River at site SJ3. The maximum value of 402.59 Bq kg^{-1} was obtained for the sample collected from site SN3 on the bank of the Neelum River. The higher value for ^{40}K could perhaps be due to the occurrence of K-feldspar within the mineral matrix of the sand deposits in the study area.

5.3 Estimation of absorbed dose rate (ADR) and total annual effective dose (AED)

For those sand samples collected from the banks of the Jhelum River, the absorbed gamma dose rate in air (nGy h^{-1}) at a point 1 m from the ground, and the annual effective dose equivalent E (mSv y^{-1}) varied from

27.32 ± 3.63 to 75.51 ± 3.74 nGy h^{-1} with a mean value of 49.88 ± 3.71 nGy h^{-1} and 0.168 ± 0.022 to 0.463 ± 0.023 mSv y^{-1} with a mean value of 0.306 ± 0.023 mSv y^{-1}, respectively (see Figs. 7, 8).

The gamma-ray absorbed dose rate in air at a point 1 m above the ground was also calculated for the samples collected from the Kunhar River and was found to range from 45.314 ± 3.917 to 75.831 ± 4.716 nGy h^{-1} with an average value of 63.311 ± 3.829 nGy h^{-1}. The value of the annual effective equivalent dose E varied from 0.278 ± 0.0240 to 0.465 ± 0.0256 mSv y^{-1}, whereas the mean value of this dose for the Kunhar River was found to be 0.388 ± 0.023 mSv y^{-1}.

The estimated value of the gamma-ray absorbed dose rate in air at a point 1 m above the ground for the samples collected from the banks of the Neelum River was found to range from 48.78 ± 3.74 to 81.46 ± 4.20 nGy h^{-1} with an average value of 64.48 ± 3.81 nGy h^{-1}. The value of the annual effective equivalent dose E was found to be in a range of 0.29 ± 0.023 to 0.49 ± 0.026 mSv y^{-1} with a mean value of 0.39 ± 0.023 mSv y^{-1}.

The total gamma-ray absorbed dose rate (GDR) in air at a point 1 m above the ground for all the studied samples was found to range from 27.324 ± 3.501 to 81.466 ± 4.2 nGy h^{-1} with an average value of 59.222 ± 3.782 nGy h^{-1}. The total annual effective equivalent dose E for the three rivers varied from 0.168 ± 0.021 to 0.5 ± 0.026 mSv y^{-1} with a mean value 0.363 ± 0.023 mSv y^{-1}.

5.4 Excess life time cancer risk (ELCR)

The gamma-ray-induced cancer risk was calculated, based on the values obtained for the annual effective dose equivalent (AEDE) and other factors, using Eq. 14.

$$\text{Excess lifetime cancer risk (ELCR)} = \text{AEDE} \times \text{Average duration of life (DL)} \times \text{Risk Factor (RF)} \quad (14)$$

where, AEDE, DL, and RF are the annual effective dose equivalent, duration of life (66 years) [42], and risk factor (Sv^{-1}), together giving the fatal cancer risk per Sievert. For low-dose background radiation which is considered to produce a stochastic effect, ICRP 60 uses values of 0.05 for public exposure [43, 44].

The ELCR defines the probability of developing cancer once over an entire lifetime for a given exposure level. ELCR due to gamma radiation exposure from sand samples varied from 0.55 × 10^{-3} to 1.65 × 10^{-3} with an average value of 1.20 × 10^{-3}. ELCR for indoor exposure was found to range from 0.44 × 10^{-3} to 1.32 × 10^{-3} with an average value of 0.96 × 10^{-3}. For outdoor exposure, ELCR varied from 0.11 × 10^{-3} to 0.33 × 10^{-3} with an average value of 0.24 × 10^{-3}.

The outdoor values of the excess lifetime cancer risk are within the recommended safety limit of 1 [43], while about 43% of the indoor excess lifetime cancer risk is slightly higher than 1. Hence, dwellers of buildings constructed using the sand addressed in the study area are at risk, to a certain degree, of developing cancer over their lifetimes.

5.5 Annual gonadal equivalent dose (AGED)

Different organs of human body, e.g., the gonads, bone marrow, and the bone surface cells, are radiosensitive. Hence, for any level of radiation exposure, these organs are vulnerable [4]. The annual gonadal dose equivalent (AGED) was calculated using the specific activities of ^{226}Ra, ^{232}Th, and ^{40}K according to Eq. 15 [45].

$$\text{AGED}\ (\mu\text{Sv}\,y^{-1}) = 3.09C_{\text{Ra}} + 4.18C_{\text{Th}} + 0.314C_{\text{K}} \quad (15)$$

where C_{Ra}, C_{Th}, and C_{K} are the specific activity concentrations of radium, thorium, and potassium, respectively. The average values of the annual gonadal equivalent dose varied from 0.191 ± 0.025 to 0.568 ± 0.029 mSv y^{-1} with an average value of 0.411 ± 0.026 mSv y^{-1}. The average value of the AGDE, resulting from gamma exposure from the sand samples, is higher than the global average value of 0.298 mSv y^{-1} reported for soil [39].

5.6 Correlation between radon exhalation rate (RER) and radium content

The correlation between the radon exhalation rate (RER) and radium content in every sand sample was investigated (see Fig. 9). The linear regression mathematical model ($Y = A + B \times X$) for the RER and ^{226}Ra content correlation is given as;

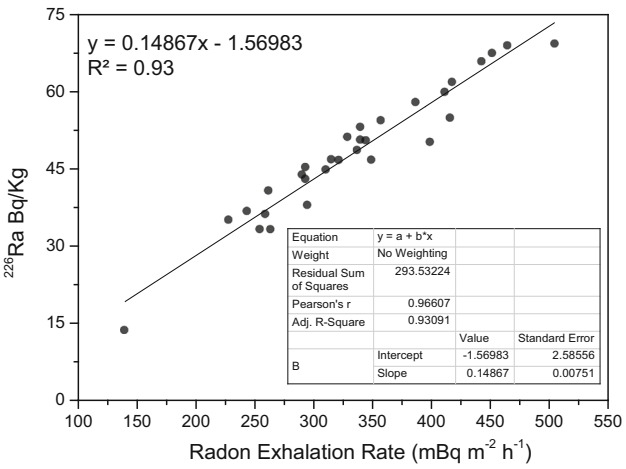

Fig. 9 Linear regression analysis of RER with ^{226}Ra

$$^{226}\text{Ra activity concentration (Bq/kg)} = 0.14867 \times \text{Value of RER} - 1.56983 \quad (16)$$

The linear correlation analysis between the RER and ^{226}Ra activity gives a slope of 0.14867 and an R^2 value of 0.93. The coefficient of determination (R^2) is a statistical measure expressing how close the data are to a fitted regression line. Wherever the radium content of a sand sample is relatively high, the RER is also high for that sample, as would be expected since ^{222}Rn is a decay product of radium, and there is a good correlation between them. A positive correlation of $R^2 = 0.93$ has been observed between the radium content and the radon exhalation rate.

5.7 Geospatial analysis

As the measurements were representative of the samples collected from a specific location, the acquisition of information about the unsampled locations would have to rely on geostatistical methods [46]. To represent the spatial distributions of the natural radionuclides concentration present in the sand samples of the study area, the Kriging interpolation method was used. The Kriging method (named after D. Krige (Krige 1966)) was further developed by Matheron (Matheron 1970) and is now regarded as being the best linear unbiased estimator (BLUE) [47]. The Kriging formula is given by Eq. 17 [46, 48];

$$Z(S_0) = \sum_{i=1}^{N} \lambda_i Z(S_i) \quad (17)$$

where $Z(S_i)$ is the estimated value at the ith place, λ_i is the unknown weight for the measured value at the ith location (ith), and S_0 is the measurement location.

For the current study, the ^{226}Ra, ^{232}Th, and ^{40}K activity concentrations are shown in Figs. 10, 11 and 12. The GDR for the current study area is shown in Fig. 13.

5.8 Normalized radionuclide concentration or equivalent multiplicative factor (EMF)

Comparisons of the results obtained in the current study with those of studies conducted in other parts of the world [11, 49–70] are shown in Figs. 14 and 15. The results of other studies are compared with those of the current study by defining the equivalent multiplicative factor (EMF) or normalized values of the radionuclide concentrations.

$$\text{Equivalent Multiplicative Factor (EMF)} = \frac{\text{Current Study Values of } ^{226}\text{Ra}, ^{232}\text{Th}, ^{40}\text{K}}{\text{Values of } ^{226}\text{Ra}, ^{232}\text{Th}, ^{40}\text{K in literature}} \quad (18)$$

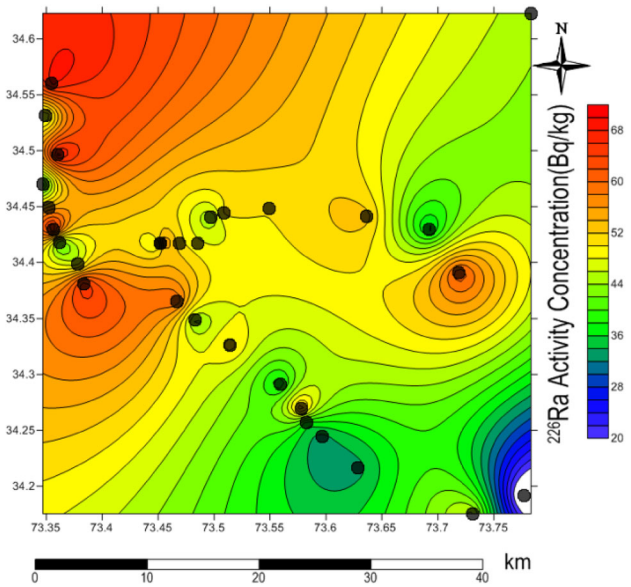

Fig. 10 (Color online) 2-D contour map of the ^{226}Ra activity concentrations obtained in the study

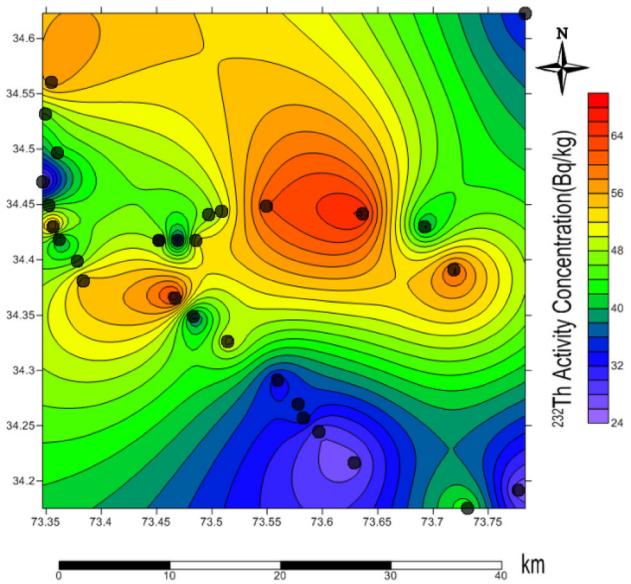

Fig. 11 (Color online) 2-D contour map for ^{232}Th activity concentrations obtained in the study

These EMF values show that the ^{226}Ra and ^{232}Th concentrations in the sand samples collected from different rivers in Muzaffarabad are somewhat higher than the data available in the literature. Similarly, the radionuclide ^{40}K equivalent multiplicative factor for the sand samples collected from different rivers in Muzaffarabad is relatively greater, but in some cases smaller, for some countries [11, 49–70].

For the majority of the analyzed sand samples, the presence of ^{40}K does not present any possible radiological

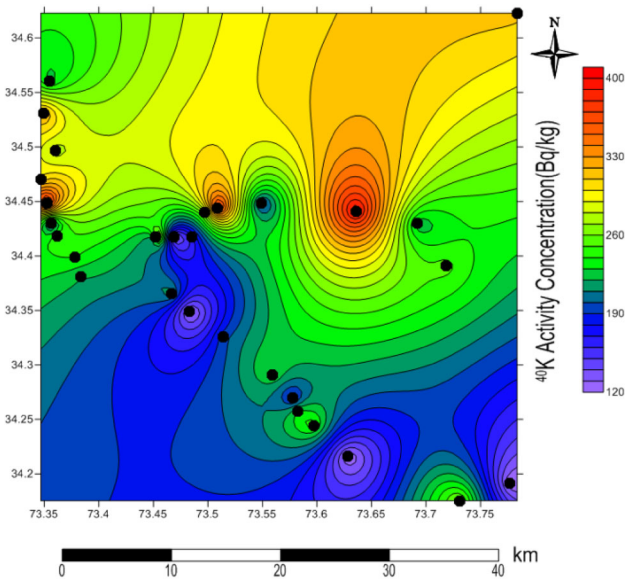

Fig. 12 (Color online) 2-D contour map for ^{40}K activity concentrations obtained in the study

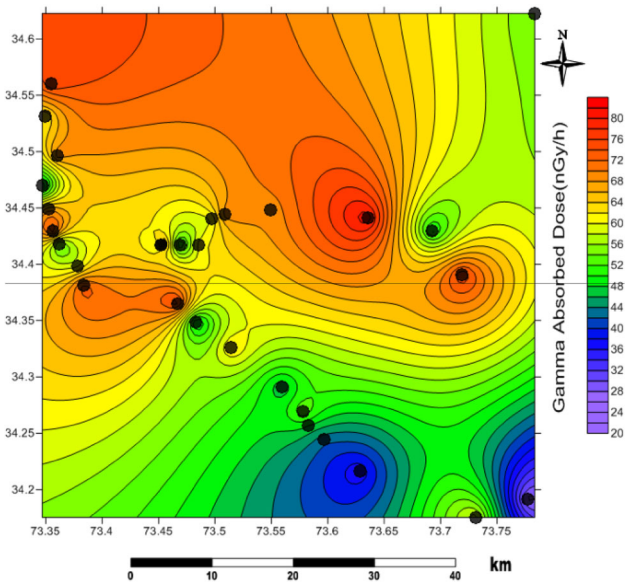

Fig. 13 (Color online) 2-D Contour map of gamma dose rate in study area

risks to human health because the concentration of ^{40}K is in a homeostatic balance with other isotopes of potassium in the atmosphere.

6 Conclusion

The NORMSs concentration and RER in sand samples with associated radiological hazards were investigated. The ELCR values for outdoor exposure were found to be within the ICRP recommended safety limit of 1, while about 43%

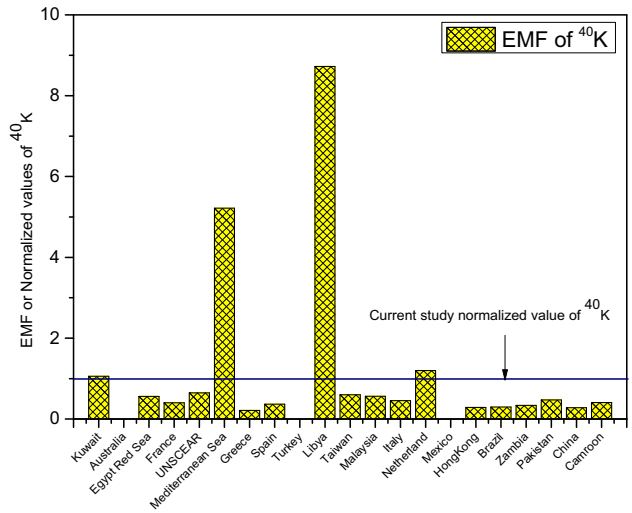

Fig. 14 Equivalent multiplicative factor (EMF) of ^{40}K for comparison with data in the literature

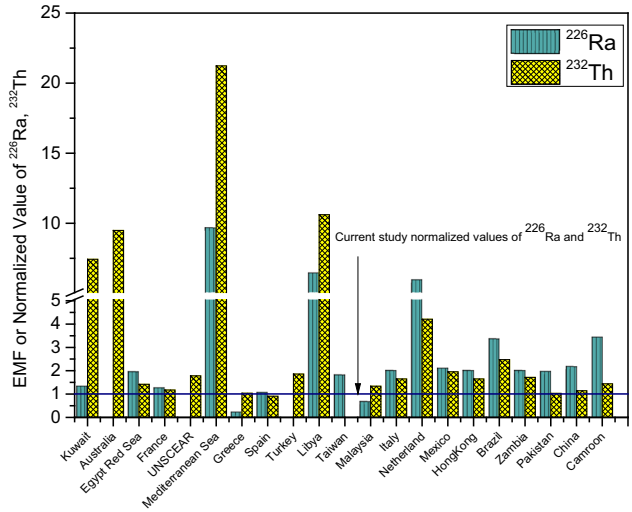

Fig. 15 (Color online) Equivalent multiplicative factor (EMF) of ^{232}Th and ^{226}Ra for comparison with data in the literature

of the samples were found to have slightly higher values than the recommended limit. On the other hand, 90% of the sand samples were found to have average AGED values, resulting from gamma exposure from the sand samples, that is higher than the world average of 0.298 mSv y^{-1} reported for soil. Furthermore, 37% of the samples were found to have a representative level index (I_r) that is slightly higher than recommended value of 1. Hence, the use of sand from the study area, given its elevated concentration of radionuclides, as a construction material requires careful regulation to minimize radiation hazards. The Ra_{eq}, external, and internal hazard indices, as well as the alpha and gamma index for the majority of the samples, were found to be less than 1, while the results for RER shows that most of the sand samples available in area can

be utilized as building materials and do not pose any significant radiation hazard to building inhabitants or other persons. It is recommended that the use of sand with high radionuclide concentrations as a construction material should be avoided.

Acknowledgements The authors gratefully acknowledge the Director General, Pakistan Institute Nuclear Science and Technology (PINSTECH), for allowing us to use their laboratories and the staff for their assistance and technical support. Mr. A. R. Khan is thankful to the Higher Education Commission of Pakistan for their awarding of a PhD Indigenous Scholarship.

References

1. NCRP, *Exposures from the Uranium Series with Emphasis on Radon and Its Daughters* (National Council on Radiation Protection and Measurements, 7910 Woodmont Avenue 1Bethesda, Report No. 77, 1984)
2. NEA-OECD, Nuclear Energy Agency. *Exposure to radiation from natural radioactivity in building materials* (Report by NEA Group of Experts, OECD, Paris, 1979)
3. UNSCEAR, *Sources, Effects and Risks of Ionizing Radiation* (United Nations Scientific Committee on the Effects of Atomic Radiation, United Nations New York, 1993)
4. UNSCEAR, *Sources and effects of ionizing radiation* (United Nations Scientific Committee on the Effects of Atomic radiation, Report to the General Assembly of the United Nations with Scientific Annexes, United Nations Sales Publication New York, 2000)
5. ECRP, Protection, *Radiological Protection Principles concerning the Natural Radioactivity of Building* (European Commission Radiation Materials Directorate-General Environment, Nuclear Safety and Civil Protection, Report 112, STUK (Finland), 1999)
6. G. Gonzalez-Chornet, J. Gonzalez-Labajo, Natural radioactivity in beach sands from Donana National Park and Mazagon (SPAIN). Radiat. Prot. Dosim. **112**, 307–310 (2004). https://doi.org/10.1093/rpd/nch3977
7. F.O. Brigido, E.N. Montalvan, Z.J. Tomas et al., Natural radioactivity in some building materials in cuba and their contribution to the indoor gamma dose rate. Radiat. Prot. Dosim. **113**, 218–222 (2005). https://doi.org/10.1093/rpd/nch434
8. N. Hizem, B.A. Fredj, L. Ghedira et al., Determination of natural radioactivity in building materials used in Tunisian dwellings by gamma ray spectrometry. Radiat. Prot. Dosim. **114**, 533–537 (2005). https://doi.org/10.1093/rpd/nch489
9. I.P. Farai, J.A. Ademola, Radium equivalent activity concentrations in concrete building blocks in eight cities in Southwestern Nigeria. J. Environ. Radioact. **79**, 119–125 (2005). https://doi.org/10.1016/j.jenvrad.2004.05.016
10. S.U. El-Kameesy, S.A. El-Ghany, Sm E-Minyawi et al., Natural radioactivity of beach sand samples in the Tripoli region. Northwest Libya Turk. J. Eng. Environ. Sci. **32**, 245–251 (2008)
11. U. Cevik, N. Damla, A.I. Koby et al., Assessment of natural radioactivity of sand used in Turkey. J. Radiol. Prot. **29**(1), 61 (2009). https://doi.org/10.1088/0952-4746/29/1/004
12. A. Jabbar, W. Arshed, A.S. Bhatti et al., Measurement of soil radioactivity levels and radiation hazard assessment in southern Rechna interfluvial region, Pakistan. Environ Mon Assess **169**, 429–438 (2010). https://doi.org/10.1007/s10661-009-1185-1
13. M. Rafique, S.U. Rahman, T. Mahmood et al., Radon exhalation rate from, soil, sand, bricks, and sedimentary samples collected from Azad Kashmir, Pakistan. Russ. Geol. Geophys. **52**, 451–458 (2011). https://doi.org/10.1016/j.rgg.2011.03.007
14. M. Rafique, H. Rehman, Matiullah et al., Assessment of radiological hazards due to soil and building materials used in Mirpur Azad Kashmir, Pakistan. Iran. J. Radiat. Res. **9**, 77–87 (2011)
15. M. Rafique, M.H. Rathore, Determination of radon exhalation from granite, dolerite and marbles decorative stones of the Azad Kashmir area, Pakistan. Int. J. Environ. Sci. Technol. **10**, 1083–1090 (2013). https://doi.org/10.1007/s13762-013-0288-y
16. M. Rafique, Ambient indoor/outdoor gamma radiation dose rates in the city and at high altitudes of Muzaffarabad (Azad Kashmir). Environ. Earth Sci. **70**, 1783–1790 (2013). https://doi.org/10.1007/s12665-013-2266-6
17. M. Rafique, M. Basharat, S. Azhar et al., Effect of geology and altitude on ambient outdoor gamma dose rates in district Poonch, Azad Kashmir. Carpathian J. Earth Environ. Sci. **8**, 165–173 (2013)
18. M. Rafique, A. Jabbar, A.R. Khan, Radiometric analysis of rock and soil samples of Leepa Valley; Azad Kashmir, Pakistan. J. Radioanal. Nucl. Chem. **298**, 2049–2056 (2013). https://doi.org/10.1007/s10967-013-2681-x
19. S.U. Rahman, F.Malik Matiullah et al., Measurement of naturally occurring/fallout radioactive elements and assessment of annual effective dose in soil samples collected from four districts of the Punjab Province Pakistan. J. Radioanal. Nucl. Chem. **287**, 647–655 (2011). https://doi.org/10.1007/s10967-010-0819-7
20. S.U. Rahman, M. Rafique, ^{232}Th, ^{226}Ra, and ^{40}K activities and associated radiological hazards in building materials of Islamabad capital territory, Pakistan. Nucl. Technol. Radiat. Prot. **27**, 392–398 (2012). https://doi.org/10.2298/NTRP1204392R21
21. S.U. Rahman, M. Rafique, A. Jabbar et al., Radiological hazards due to naturally occurring radionuclides in the selected building materials used for the construction of dwellings in four districts of the Punjab province, Pakistan. Radiat. Prot. Dosim. **153**, 352–360 (2013). https://doi.org/10.1093/rpd/ncs109
22. M.A. Baloch, A.A. Qureshi, A. Waheed et al., A study on natural radioactivity in Khewra salt mines, Pakistan. J. Radiat. Res. **53**, 411–421 (2012). https://doi.org/10.1269/jrr.11162
23. X. Ding, X. Lu, C. Zhao et al., Measurement of natural radioactivity in building materials used in Urumqi, China. Radiat. Prot. Dosim. **155**, 374–379 (2013). https://doi.org/10.1093/rpd/nct002
24. M.A. Arnedo, A. Tejera, J.G. Rubiano et al., Natural radioactivity measurements of beach sands in Gran Canaria, Canary Islands (Spain). Radiat. Prot. Dosim. **156**, 75–86 (2013). https://doi.org/10.1093/rpd/nct044
25. A.A. Qureshi, I.A.K. Jadoon, A.A. Wajid et al., Study of natural radioactivity in mansehra granite, Pakistan: environmental concerns. Radiat. Prot. Dosim. **158**, 466–478 (2014). https://doi.org/10.1093/rpd/nct271
26. BEIR VI, *Health Effects of Exposure to Radon* (National Academy Press, Washington, DC, 1999)
27. Y. Sakoda, Y. Ishimori, A comprehensive review of radon emanation measurements for mineral, rock, soil, mill tailing and fly ash. Appl. Radiat. Isot. **69**, 1422–1435 (2011)
28. J.M. Stajic, D. Nikezic, Theoretical calculation of radon emanation fraction. Nucl. Instrum. Methods Phys. Res. B **336**, 19–25 (2014). https://doi.org/10.1016/j.nimb.2014.06.013
29. T. Sasaki, Y. Gunji, T. Okuda, Demonstration of a method to suppress radon emanation from uranium bearing wastes. Nucl. Sci. Technol. **41**, 843–849 (2004). https://doi.org/10.1080/18811248.2004.9715555
30. C. Duenas, M.C. Fernandez, J. Carretero et al., Release of ^{222}Rn from some soils. Ann. Geophys. **15**(1), 124–133 (1997). https://doi.org/10.1007/s00585-997-0124-0

31. S.A. Durrani, R. Ilic, *Radon measurements by Etched Track Detectors* (World Scientific, London, 1997)
32. S. Rehman, S.Rehman Matiullah et al., Studying ^{222}Rn exhalation rate from soil and sand samples using CR-39 detector. Radiat. Meas. **41**(6), 708–713 (2006). https://doi.org/10.1016/j.radmeas.2006.03.005
33. K. Debertin, F.G. Helmer, *Gamma and X-ray Spectrometry with Semiconductor Detectors* (North Holland, Amsterdam, 1988)
34. G. Heusser, H.V. Klapdor, A. Ptepki et al., Construction of a low-level Ge detector. Appl. Radiat. Isot. **40**, 393 (1989). https://doi.org/10.1016/0883-2889(89)90203-7
35. W. Westmeier, Techniques and problems of low level gamma ray spectrometry. Appl. Radiat. Isot. **43**, 305 (1992). https://doi.org/10.1016/0883-2889(92)90102-K
36. A.B. Fredj, N. Hizem, M. Chelbi et al., Quantitative analysis of gamma-ray emitters radioisotopes in commercialized bottled water in Tunisia. Radiat. Prot. Dosim **117**(4), 419–424 (2005). https://doi.org/10.1093/rpd/nci315
37. J. Beretka, P.J. Mathew, Natural radioactivity of Australian building materials, industrial wastes and by-products. Health Phys. **48**, 87–95 (1985)
38. S. Righi, L. Bruzzi, Natural radioactivity and radon exhalation in building materials used in Italian dwellings. Environ. Radioact. **88**, 158–570 (2006). https://doi.org/10.1016/j.jenvrad.2006.01.009
39. L. Xinwei, W. Lingqing, J. Xiaodan et al., Specific activity and hazards of Archeozoic-Cambrian rock samples collected from the Weibei area of Shaanxi, China. Radiat. Prot. Dosim. **118**(3), 352–359 (2006). https://doi.org/10.1093/rpd/nci339
40. UNSCEAR, *Sources and effects of ionizing radiation* (United Nations Scientific Committee on the effects of atomic radiation, New York, United Nations, 1988)
41. Matiullah Determination of the calibration factor for, CR-39 based indoor radon detector. J. Radioanal. Nucl. Chem. **298**(1), 369–373 (2013). https://doi.org/10.1007/s10967-013-2451-9
42. M. Rafique, S.U. Rahman, M. Basharat et al., Evaluation of excess life time cancer risk from gamma dose rates in Jhelum valley. J. Radiat. Res. Appl. Sci. **7**(1), 28–35 (2014). https://doi.org/10.1016/j.jrras.2013.11.005
43. ICRP, International Commission on Radiological Protection (ICRP Publication 60. Elmsford, NY, Pergamon, 1991)
44. H. Taskin, M. Karavus, P. Topuzoglu et al., Radionuclide concentrations in soil and lifetime cancer risk due to the gamma radioactivity in Kirklareli, Turkey. J. Environ. Radioact. **100**, 49–53 (2009). https://doi.org/10.1016/j.jenvrad.2008.10.012
45. M. Tufail, A. Nasim, M. Waqas et al., Measurement of terrestrial radiation for assessment of gamma dose from cultivated and barren saline soils of Faisalabad in Pakistan. Radiat. Meas. **41**(4), 443–451 (2006). https://doi.org/10.1016/j.radmeas.2005.10.007
46. M. Armstrong, *Basic Linear Geostatistics* (Springer, Berlin, 1998). http://books.google.com/books?id=_9vp11VuMCsC&pgis=1
47. D.D. Sarma, *Geostatistics with Applications in Earth Sciences*, 2nd edn. (Springer, Dordrecht, 2009). https://doi.org/10.1007/978-1-4020-9380-7
48. T. Dindaroğlu, The use of the GIS Kriging technique to determine the spatial changes of natural radionuclide concentrations in soil and forest cover. J. Environ. Health Sci. Eng. **12**, 1–11 (2014). https://doi.org/10.1186/s40201-014-0130-6
49. A. Baeza, M. Del Rio, C. Miro et al., Natural radioactivity in soils in the province of Caceres (Spain). Radiat. Prot. Dosim. **45**(1), 261–263 (1992). https://doi.org/10.1093/oxfordjournals.rpd.a081539
50. J.G. Ackers, J.F. Den-Boer, P. De-Jong et al., Radioactivity and radon exhalation rates of building materials in the Netherlands. Sci. Total Environ. **45**, 151–156 (1985). https://doi.org/10.1016/0048-9697(85)90215-3
51. A. Buttaglia, L. Bramati, Environmental radiation survey around a cool-fired power plant site. Radiat. Prot. Dosim. **24**, 407–410 (1988)
52. T.Y. Chang, W.L. Cheng, P.S. Weng, Potassium uranium, and thorium contents in building material of Taiwan. Health Phys. **27**, 385–387 (1974)
53. S. Chong, G.U. Ahmad, Gamma activity of some building materials in west Malaysia. Health Phys. **43**(2), 272–273 (1982)
54. M. Chung-Keung, L. Shun-Yin, A. Shui-Chun et al., Radionuclide contents in building materials used in Hong Kong. Health Phys. **57**(3), 397–401 (1989)
55. M.H. El-Mamoney, A.E.M. Khater, Environmental characterization and radio-ecological impacts of non-nuclear industries on the red sea coast. Environ. Radiol. **73**(2), 151–168 (2004). https://doi.org/10.1016/j.jenvrad.2003.08.008
56. G. Espinosa, J.I. Golzarri, I. Gamboa et al., Natural radioactivity in Mexican building material by SSNTD. Nucl. Trac. Radiat. Meas. **12**, 767–770 (1986). https://doi.org/10.1016/1359-0189(86)90699-0
57. P. Hayumbu, M.B. Zaman, N.C.H. Lubaba et al., Natural radioactivity in Zambian building materials collected from Lusaka. J. Radioanal. Nucl. Chem. **199**(3), 229–238 (1995). https://doi.org/10.1007/BF02162371
58. R.H. Higgy, Natural radionuclides and plutonium isotopes in soil and shore sediments on alexandria mediterranean sea coast of Egypt. Radiol. Chim. Acta **88**(1), 47–57 (2000). https://doi.org/10.1524/ract.2000.88.1.047
59. M.N. Kumru, Possible Uranium Rich in the Aegean Region of Turkey. Appl. Radiat. Isot. **48**, 295–299 (1997). https://doi.org/10.1016/S0969-8043(96)00047-4
60. K. Khalid, P. Akhter, S.D. Orfi et al., Estimation of radiation doses associated with natural radioactivity in sand samples of the North-Western Areas of Pakistan Using Monte Carlo Simulation. J. Radioanal. Nucl. Chem. **265**(3), 371–375 (2005). https://doi.org/10.1007/s10967-005-0835-1
61. A. Lambrechts, L. Foulquier, J. Garnier-Laplace et al., Natural radioactivity in the aquatic component of the main French rivers. Radiat. Prot. Dosim. **45**, 253–256 (1992). https://doi.org/10.1093/rpd/45.1-4.253
62. X.W. Lu, X.L. Zhang, Measurement of natural radioactivity in sand samples collected from the Baoji Weihe Sands Park, China. Environ. Geol. **50**(7), 977–982 (2006). https://doi.org/10.1007/s00254-006-0266-5
63. A. Malanca, V. Pessina, G. Dallara et al., Radionuclide content of building materials and gamma ray dose rates in dwellings of Rio Grande Do Norte, Brazil. Radiol. Prot. Dosim. **48**(2), 199–203 (1993). https://doi.org/10.1093/oxfordjournals.rpd.a081865
64. R.J. Meijer, I.R. James, P.J. Jennings et al., Cluster analysis of radionuclide concentrations in beach sand. Appl. Radiat. Isot. **54**, 535–542 (2001). https://doi.org/10.1016/S0969-8043(00)00196-2
65. S. Stoulos, M. Manolopoulou, C. Papastefanou et al., Assessment of natural radiation exposure and radon exhalation from building materials in Greece. J. Environ. Radiol. **69**(3), 225–240 (2003). https://doi.org/10.1016/S0265-931X(03)00081-X
66. M. Ngachin, M. Garavaglia, C. Giovani et al., Assessment of natural radioactivity and associated radiation hazards in some Cameroonian building materials. Radio Meas. **42**(1), 61–67 (2007). https://doi.org/10.1016/j.radmeas.2006.07.007
67. S.Y. Omar, *Determination of the Concentration of Natural and Man-Made Radioactivity in the Northeast Region of Libya*, Ph.D. thesis. Faculty of Science Cairo University (1997)
68. H.R. Saad, D. Al-Azmi, Radioactivity concentrations in sediments and their correlation to the coastal structure in Kuwait.

Appl. Radiat. Isot. **56**(6), 991–997 (2002). https://doi.org/10.1016/S0969-8043(02)00061-1

69. G. Sciocchetti, F. Scacco, P.G. Baldassini et al., Indoor measurements of airborne natural radioactivity in Italy. Radiat. Prot. Dosim. **7**, 347–351 (1984). https://doi.org/10.1093/oxfordjournals.rpd.a083025
70. G. Travidon, H. Flouro, A. Angelopoulos et al., Environmental Study of the Radioactivity of the Spas in the Island of Ikaria, Greece. Radiat. Prot. Dosim. **63**, 63–67 (1996). https://doi.org/10.1093/oxfordjournals.rpd.a031513